

Supporting Information for:

Structure and Chemical Stability in Perovskite-Polymer Hybrid Photovoltaic Materials

*Daniel J. Fairfield,¹ Hiroaki Sai,¹ Ashwin Narayanan,¹ James V. Passarelli,² Michelle Chen,²
Joseph Palasz,² Liam C. Palmer,^{2,4} Michael R. Wasielewski,² and Samuel I. Stupp^{*1,2,3,4,5}*

¹Department of Materials Science and Engineering, Northwestern University, Evanston, Illinois 60208, USA, ²Department of Chemistry, Northwestern University, Evanston, Illinois 60208, USA, ³Department of Medicine, Northwestern University, Chicago, Illinois 60611, USA, ⁴Simpson Querrey Institute, Northwestern University, Chicago, Illinois 60611, ⁵Department of Biomedical Engineering, Northwestern University, Evanston, IL 60208, USA.

[*s-stupp@northwestern.edu](mailto:s-stupp@northwestern.edu)

Detailed device fabrication procedure:

Patterned ITO substrates were scrubbed with soap before being sonicated in hexanes, soap solution, milli-Q water, and 1:1:1 Acetone/Methanol/Isopropanol sequentially. The substrates were then dried under a stream of nitrogen gas and subject to UV-Ozone cleaning. PEDOT-PSS was deposited on the substrates by spin coating at 5000 rpm for 60 seconds with a 5 second ramp followed by a 25-minute heating at 150 Celsius.

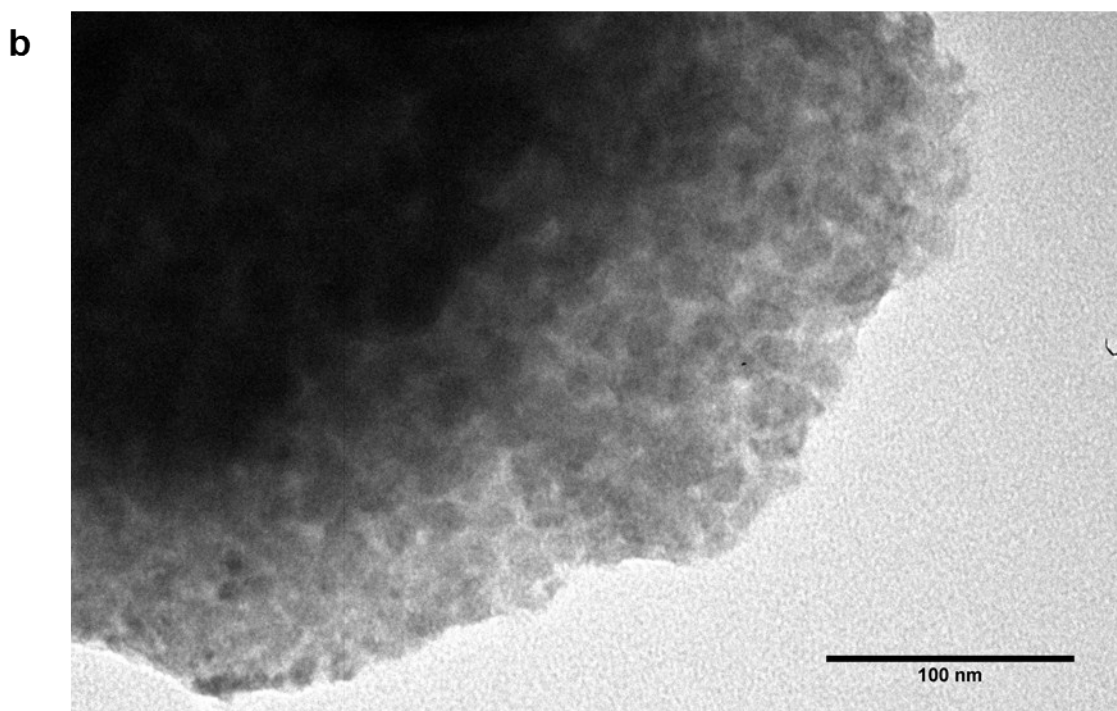
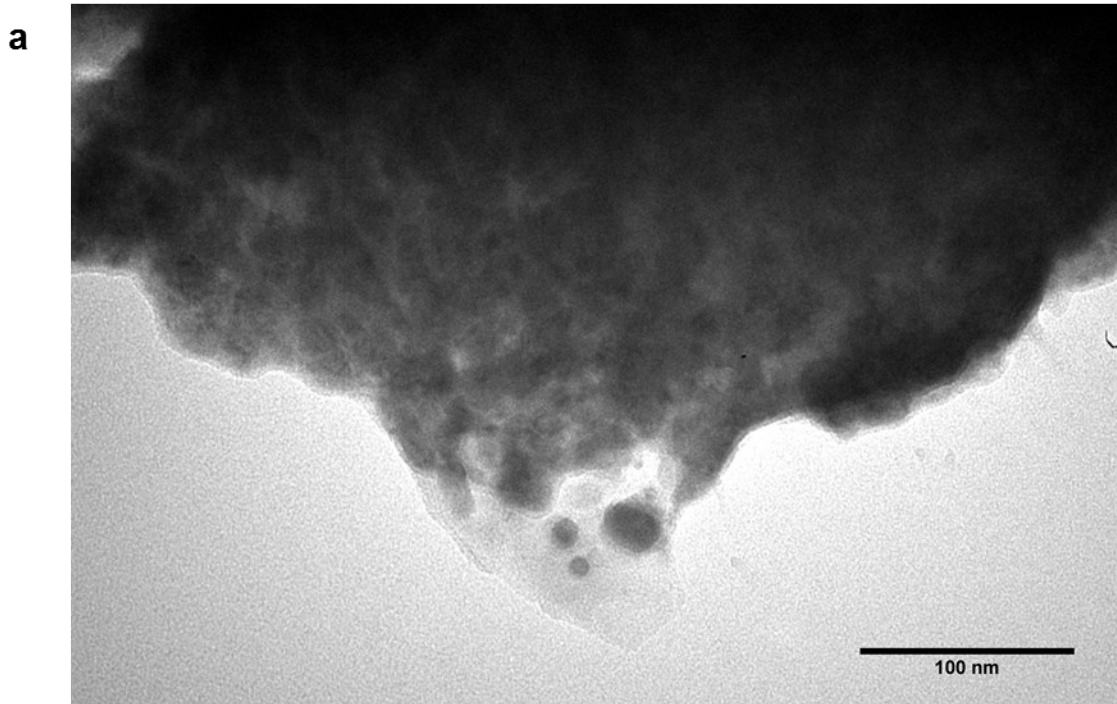
For controls

The perovskite active layer was prepared by spin coating a 36 weight % solution of perovskite in a 7 to 3 mixture of γ -butyrolactone (GBL) and dimethyl sulfoxide (DMSO) at 1000 rpm for 10 seconds with a 5 second ramp followed by 5000 rpm for 20 seconds with a 2 second ramp. After the substrate had been spinning for 15 seconds at 5000 rpm 900 mL of dry toluene was dropped onto the film before the spin program completed. The films were then annealed at 120C for 10 minutes and left to dry overnight under vacuum.

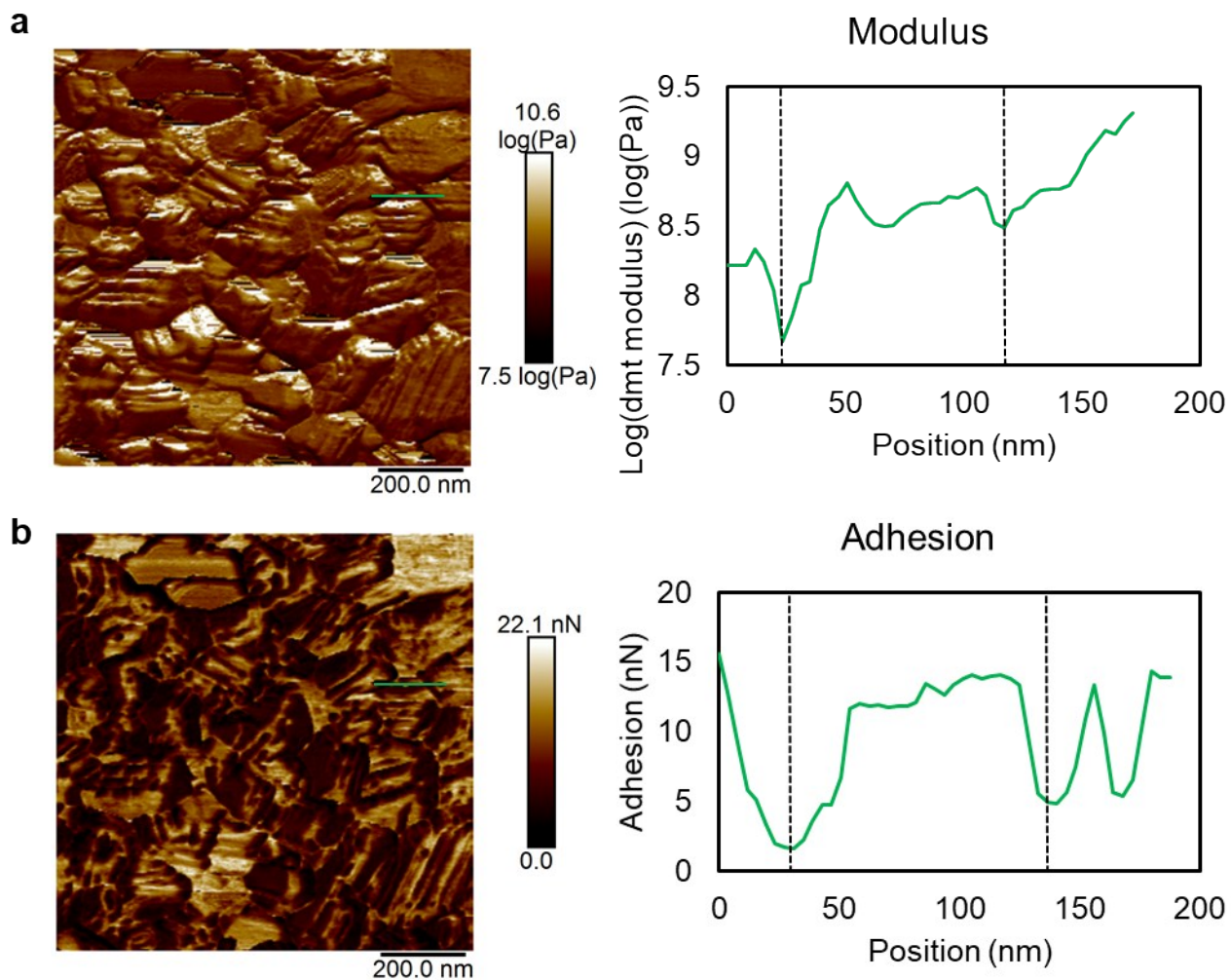
For polymer cells

The blended polyacrylic acid/perovskite active layers were prepared by spin coating from a solution that was 4 parts the stock perovskite solution mentioned above and 1 part 40mg/ml 250k polyacrylic acid in 4:1 DMF: DMSO. This solution was then diluted to 2.4x the original volume to maintain appropriate thickness for functional devices. The spin program features first spinning at 1000 rpm for 10 seconds with a 5 second ramp followed by 60 seconds at 4000 rpm with a 2 second ramp. Toluene was dropped on these films 20 seconds after the films had accelerated to 4000 rpm. The films were then annealed at 100C for 30 minutes and left to dry overnight under vacuum.

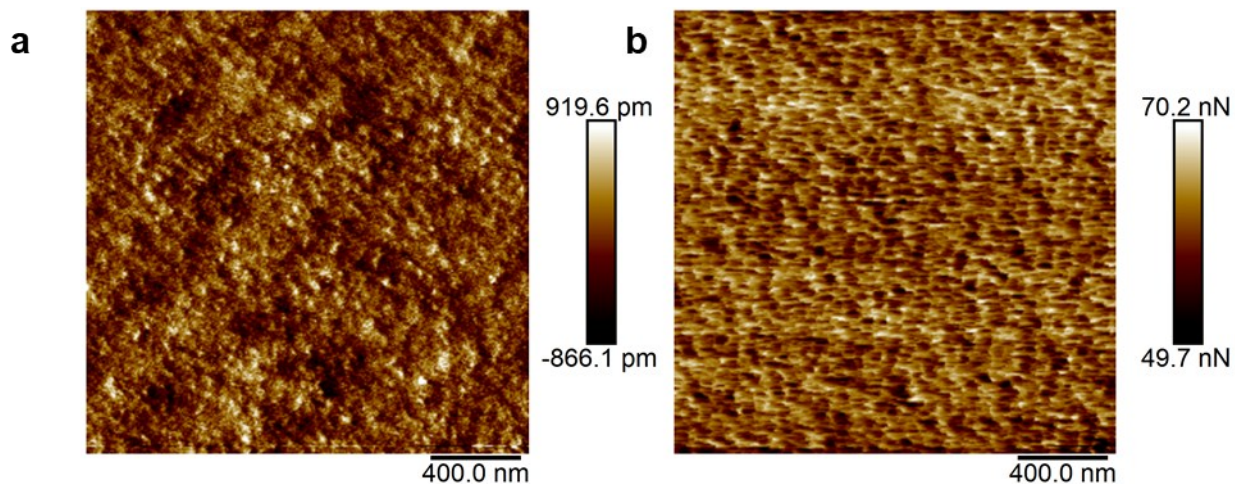
Following drying PCBM was spun onto the active layers from an 8mg/ml solution in chlorobenzene at 1200 rpm for 40 seconds with a 5 second ramp. After allowing 30 minutes to ensure the films are completely dry, bathocuproine was spun onto the films from a .5 mg/ml solution in ethanol at 5000 rpm (already spinning) for 60 seconds. Gold was then deposited as the top contact using a thermal evaporator inside an MBraun glovebox.



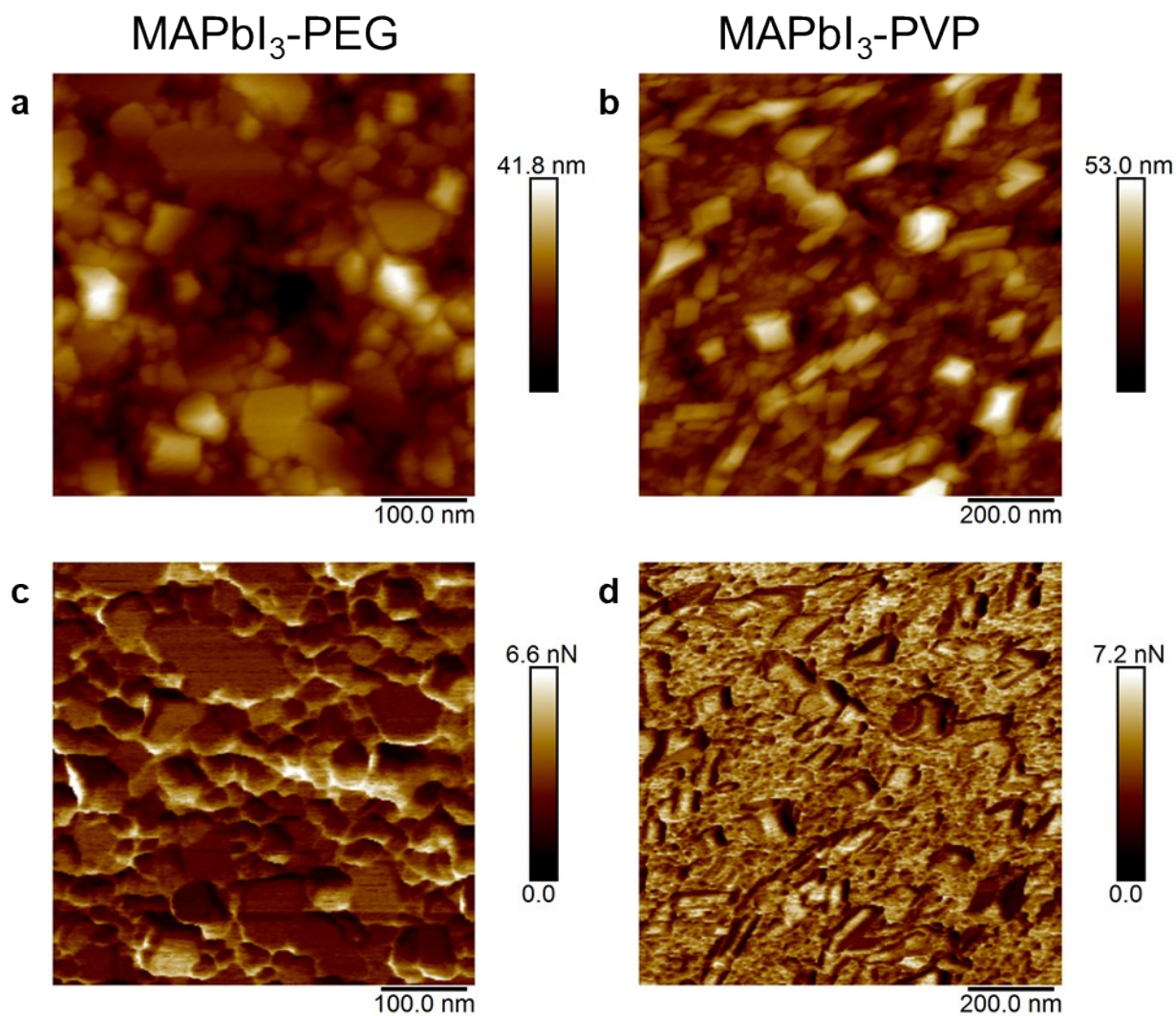
SI Figure 1. TEM micrographs of a 15:1 MAPbI₃-PAA sample showing perovskite and polymer phase separation



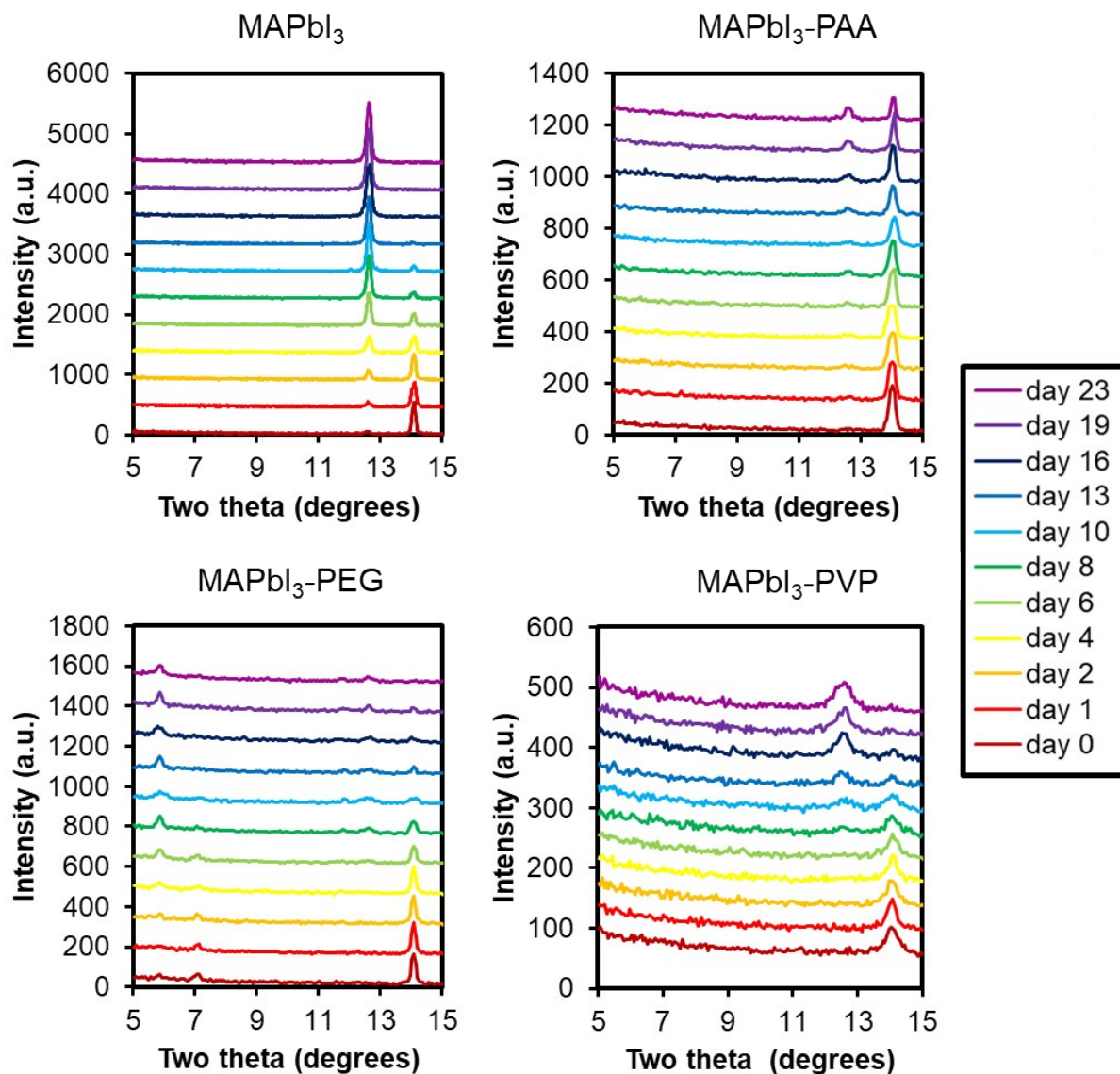
SI figure 2. Log(modulus) (a) and adhesion (b) line cuts of nanomechanical AFM data MAPbI₃ film are shown. The green lines indicate where the line cuts were taken on the AFM data, and dashed lines on the graphs correspond to where the line cuts intersected with grain boundaries. This data indicates that for the control MAPbI₃ samples the modulus and adhesion tend to be at local minima at the grain boundaries.



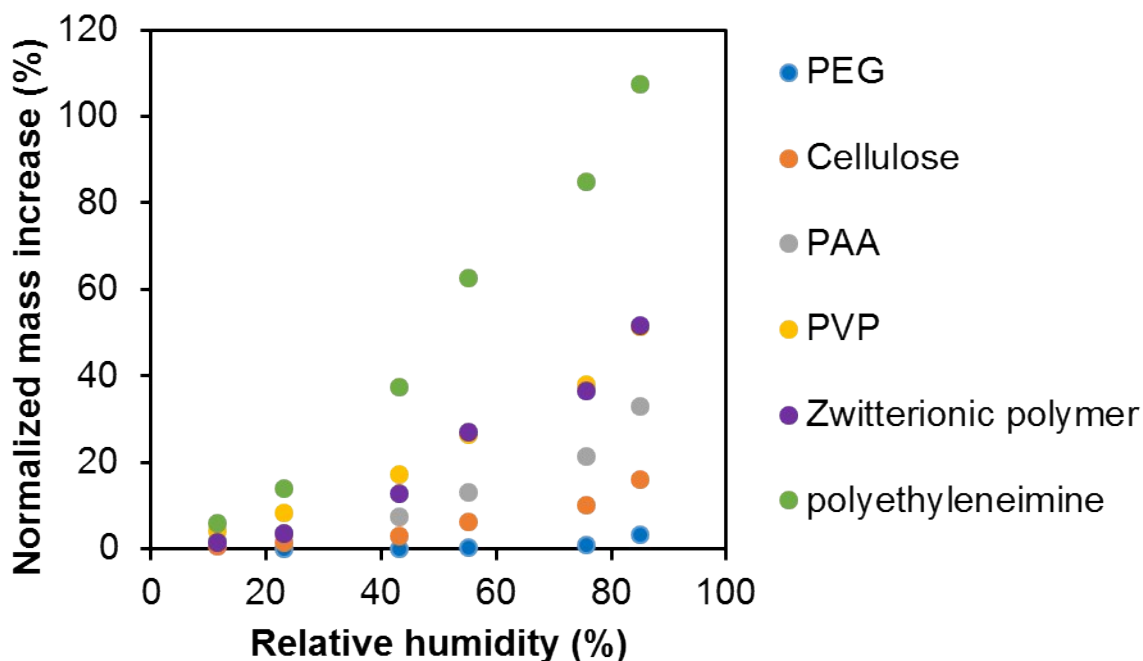
SI figure 3. Nanomechanical AFM micrographs of (a) height and (b) adhesion of a neat poly(acrylic) acid film on glass. The polymer film is extremely smooth, and adhesion to the AFM cantilever is significantly higher than what we observe for the perovskite (figure 3c).



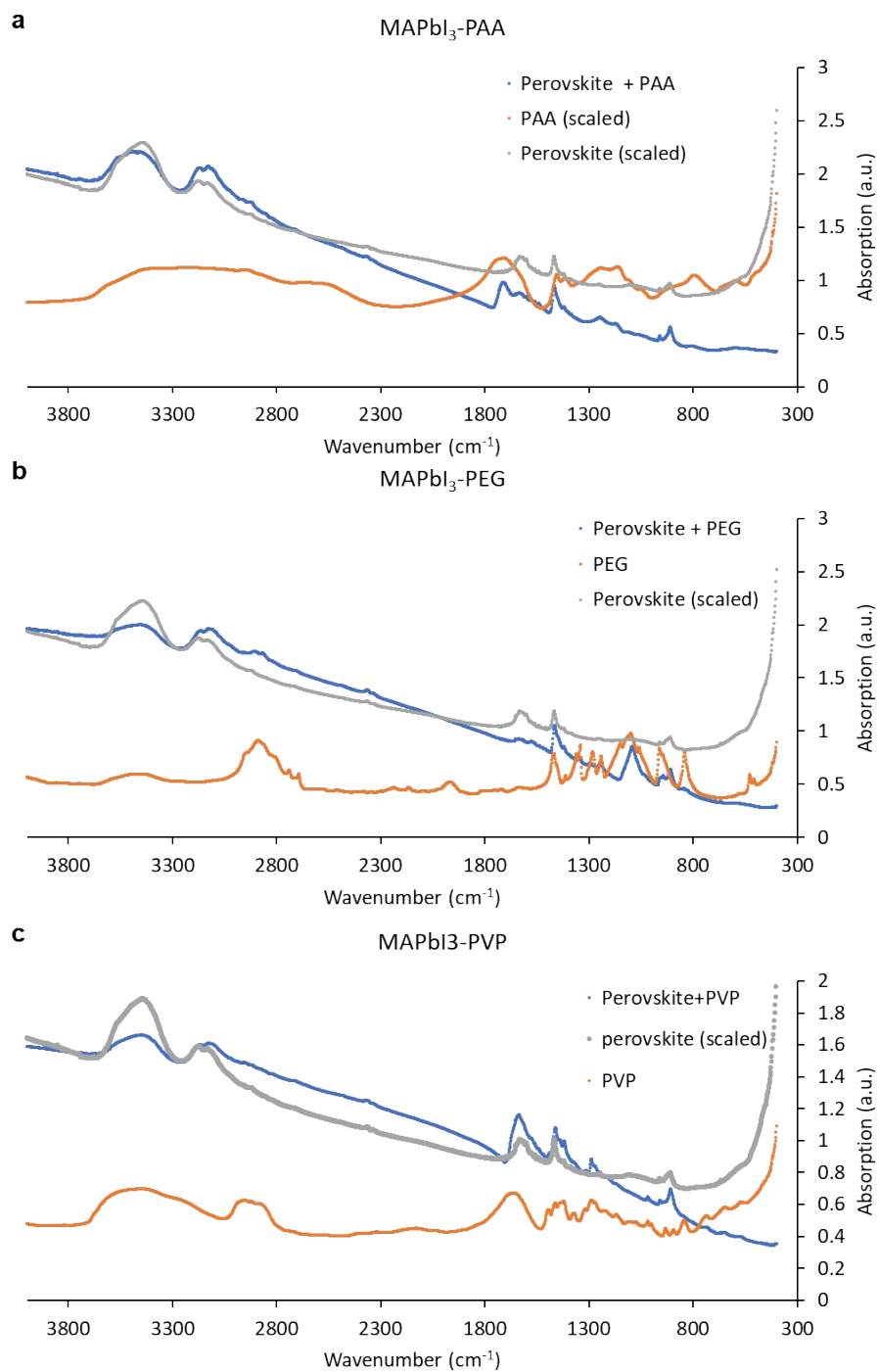
SI figure 4. Nanomechanical AFM height (a, b) and adhesion (c, d) maps of MAPbI₃-PEG (a, c) and MAPbI₃-PVP (b, d).



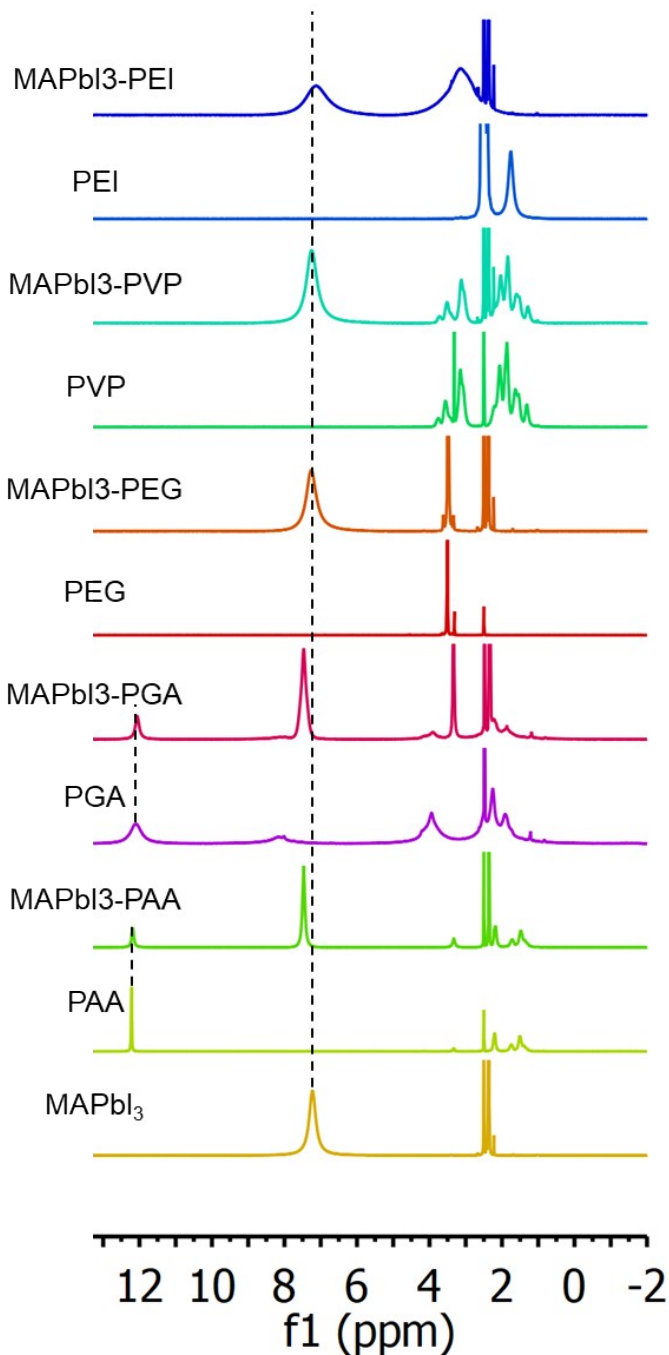
SI Figure 5. XRD of MAPbI₃ and MAPbI₃-polymer hybrid films aged at 43%RH under illumination. MAPbI₃ degraded to PbI₂ (12°) entirely within the first 10 days. MAPbI₃-PAA degraded much more slowly and retained some perovskite signal (14°) throughout the duration of the experiment. MAPbI₃-PEG degraded about as quickly as MAPbI₃, but it did not form strongly crystalline PbI₂. Finally, MAPbI₃-PVP degraded a bit more slowly than the control to form PbI₂, but overall, the crystallinity of the MAPbI₃-PVP sample was lower.



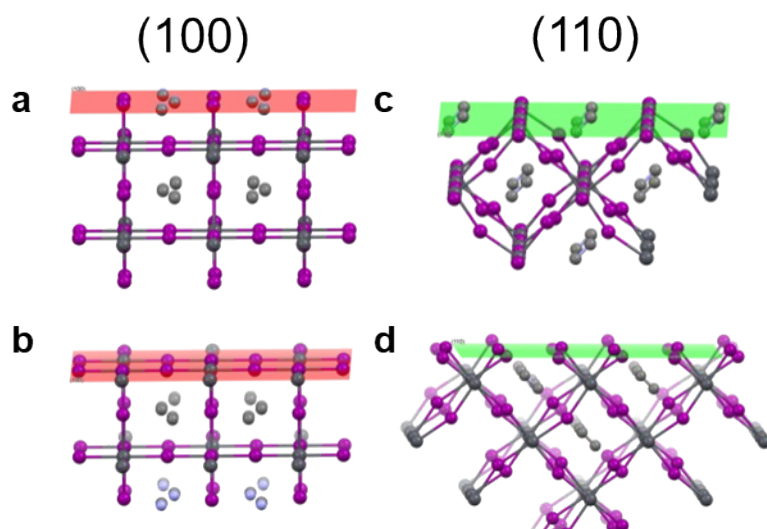
SI figure 6. Plot shows the amount of water absorbed by various polymers at a range of humidity levels. One of the previously proposed mechanisms for enhanced stability in perovskite polymer hybrid films was that the amount of water absorbed by the polymer would correspond to the enhancement of the stability of the device¹⁶. To test this hypothesis, we first measured the amount of water absorbed by various bulk polymer samples at different humidity levels. The figure shows that the polymers we tested absorbed 10 wt% to 70 wt% water compared to their original dehydrated mass over the course of a day. After several days, we re-measured the mass of these polymers and found that they were already saturated and thus did not absorb more water at later time points. Given that these polymers absorb so much water; one would expect that the amount of water absorbed would correspond to either added or reduced stability in the films. However, our film stability tests show that there isn't any correlation between absorption of water in the polymer and stability in the films. If water absorption alone is the reason for improved stability of these devices, then the hybrid perovskite polymer film stability should correspond to the absorption we observe in the polymers. However, what we find instead is that specific polymers work to enhance the stability of the perovskite independently of how much water they absorb.



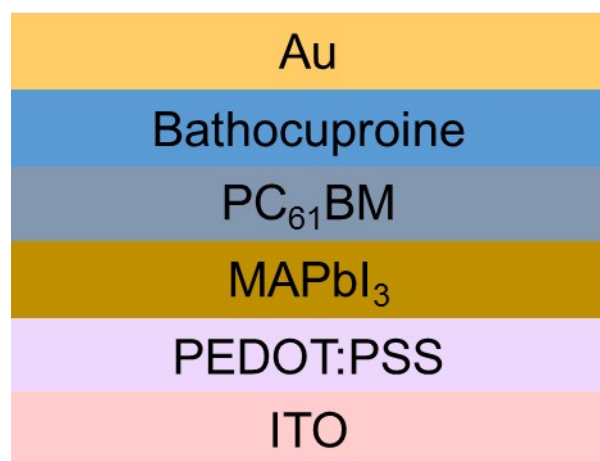
SI figure 7. Fourier-transform Infrared spectroscopy (FT-IR) was performed on powders of perovskite-polymer hybrids to compare to perovskite and polymers separately. While there were some shifts present in the data, many of the differences in the combined samples could be attributed either to convolution of perovskite and polymer peaks, or to dilution effects. We do observe the shift noted in Guo et al (ref 19) at 1660 cm^{-1} corresponding to the amide C=O bond loosening, however in our case that peak overlaps strongly with the perovskite signal. Thus, we may have at least some evidence that there is an h-bonding interaction between the PVP and the ammonium proton on the methylammonium.



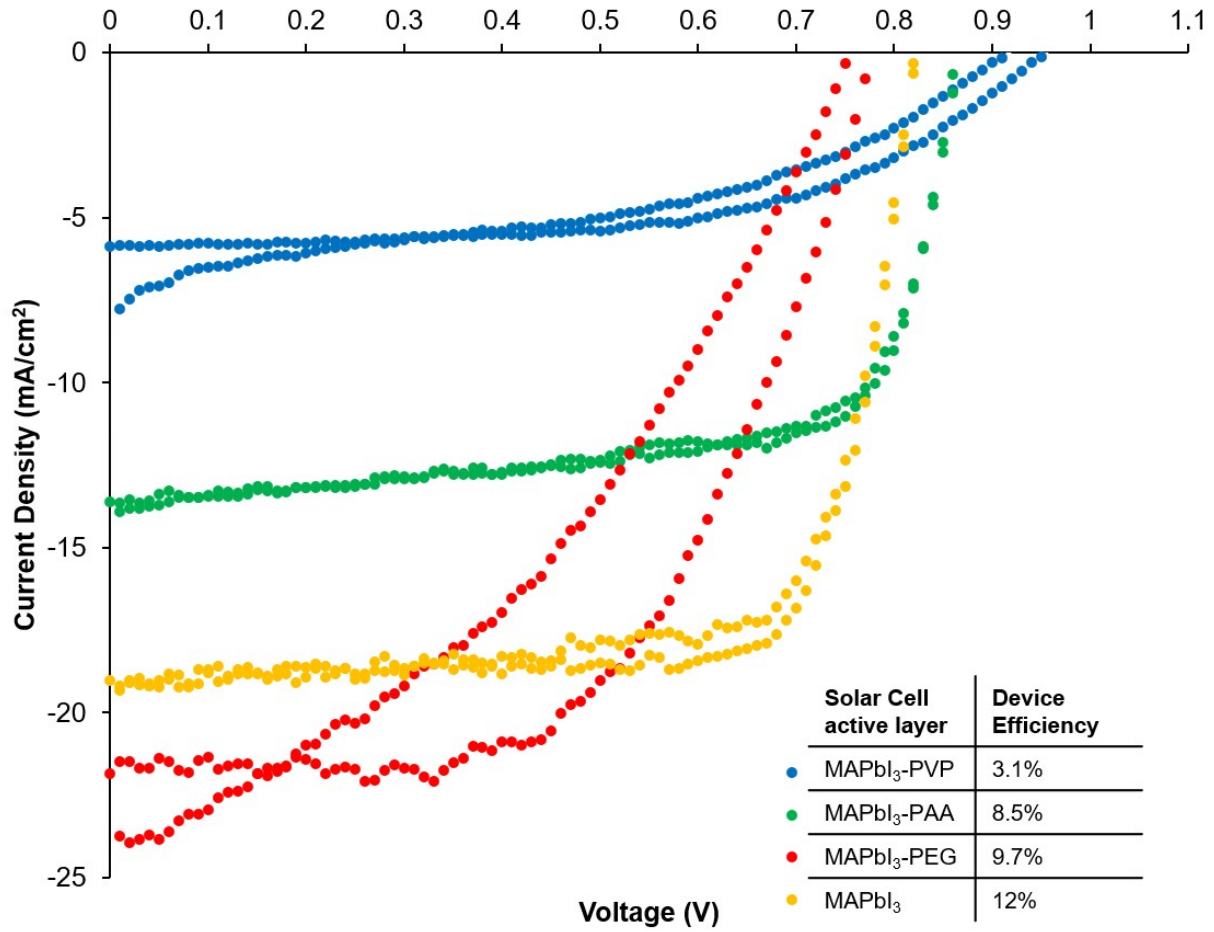
SI figure 8. NMR spectra of the perovskite precursor solution and perovskite-polymer precursor solutions compared to polymers alone in DMSO-*d*₆. The dashed lines at 7.2 ppm and 12.1 ppm are included to show the relative shifts in the ammonium protons and carboxylic acid protons, respectively. It is clear that the carboxylic acid peaks on the polymers shift upfield when mixed with the perovskite precursors and the ammonium proton peaks shift downfield, indicating hydrogen bonding between the two functional groups.



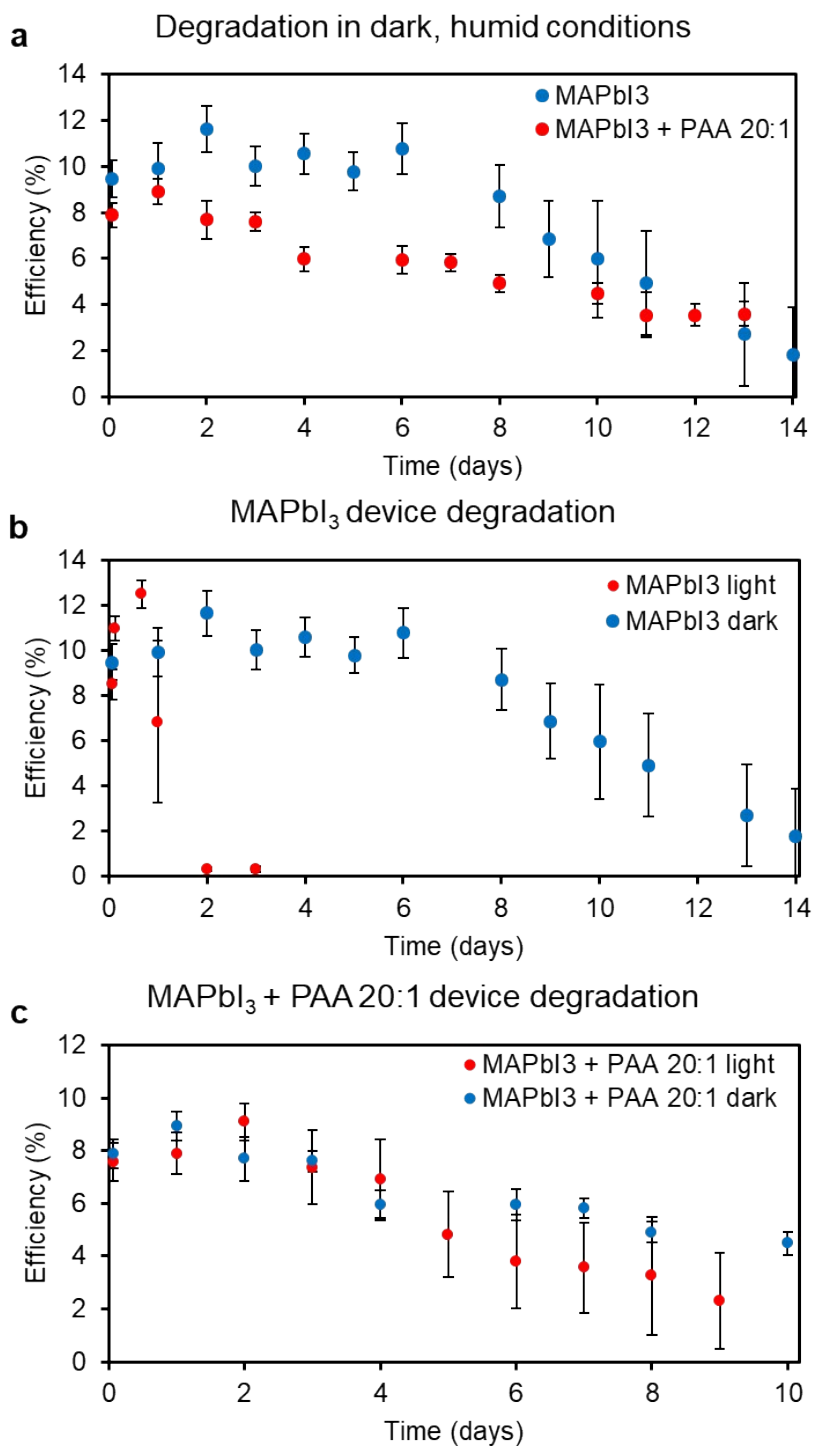
SI figure 9. Cuts of the MAPbI₃ crystal along the (a,b) (100) and (c,d) (110) planes showing the surface termination atoms along those planes at different depths in the unit cell.



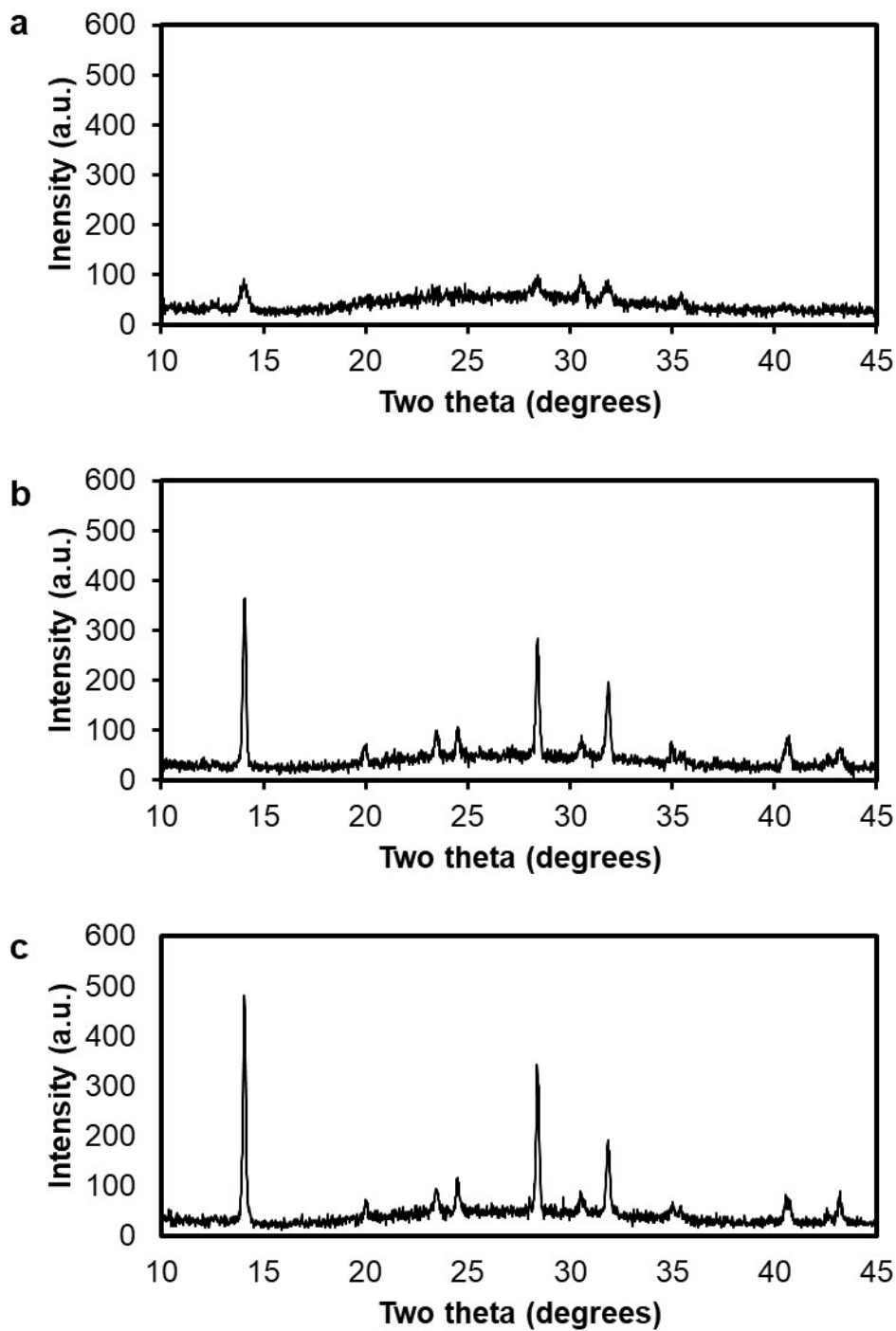
SI Figure 10. A schematic cross-section of our devices used for stability testing



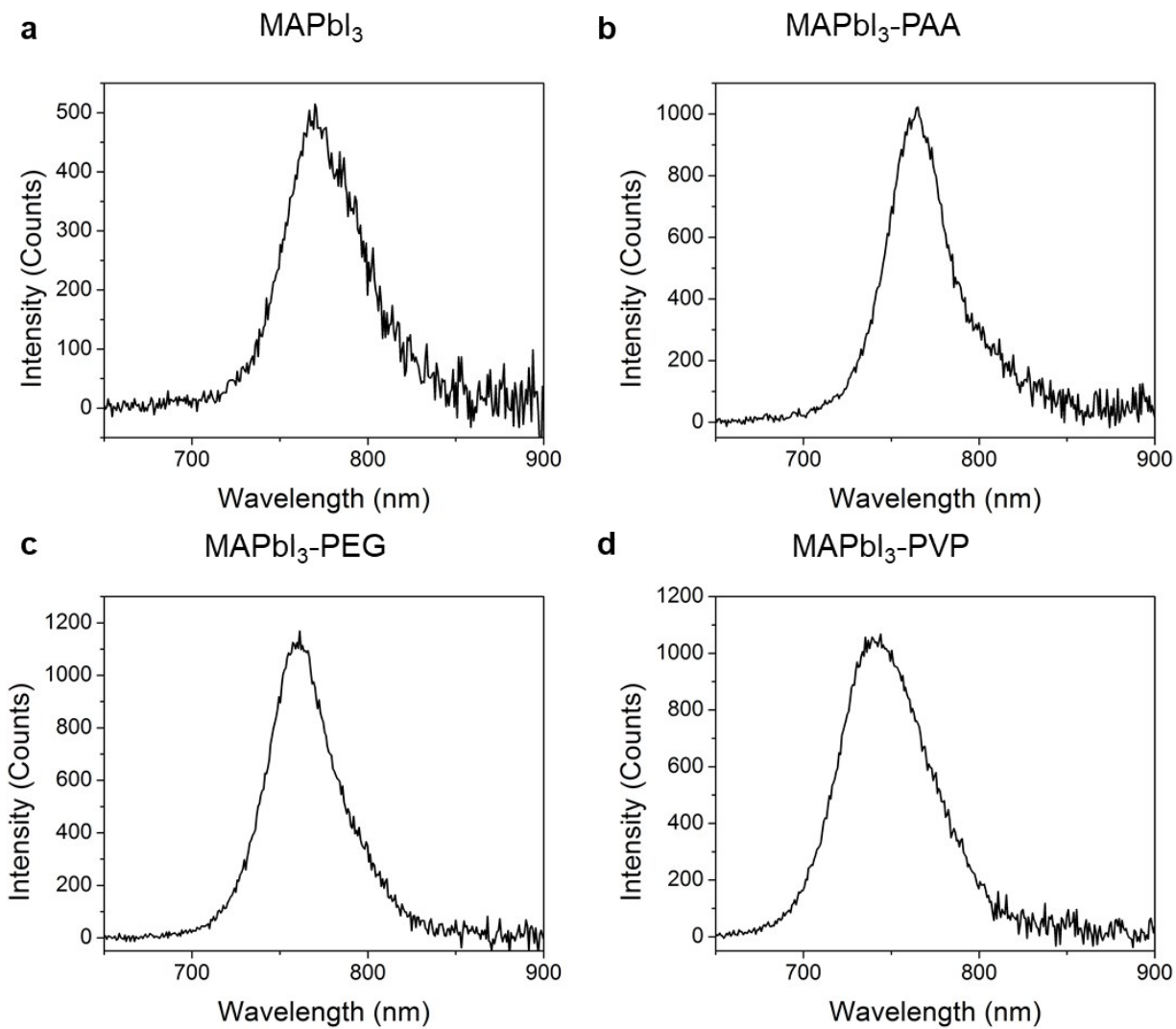
SI figure 11. Representative J-V curves for various perovskite-polymer hybrid solar cells



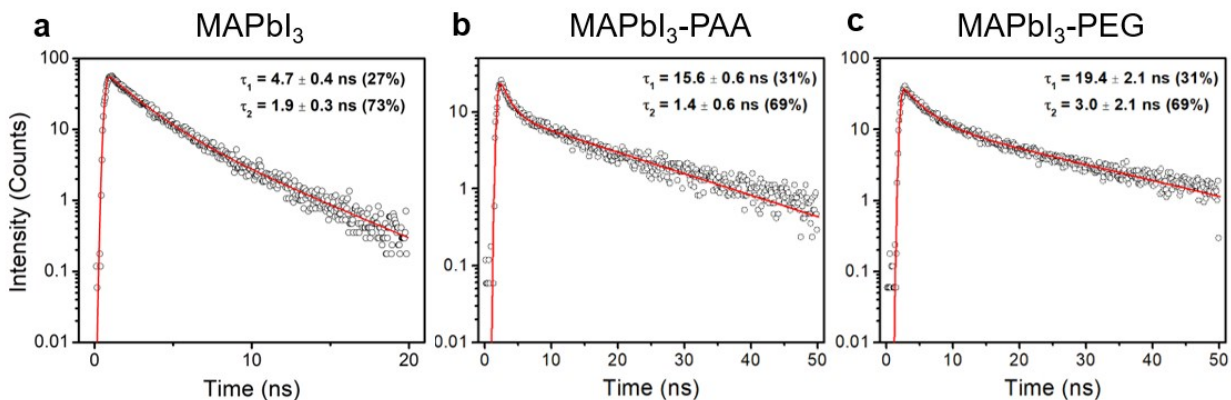
SI figure 12. Perovskite solar cell stability over time a) under 43% relative humidity in air in the dark. Device stability is then compared between light and dark conditions under 43% relative humidity for b) MAPbI₃ devices and c) MAPbI₃-PAA devices. Error bars indicate standard deviation across n=7 devices.



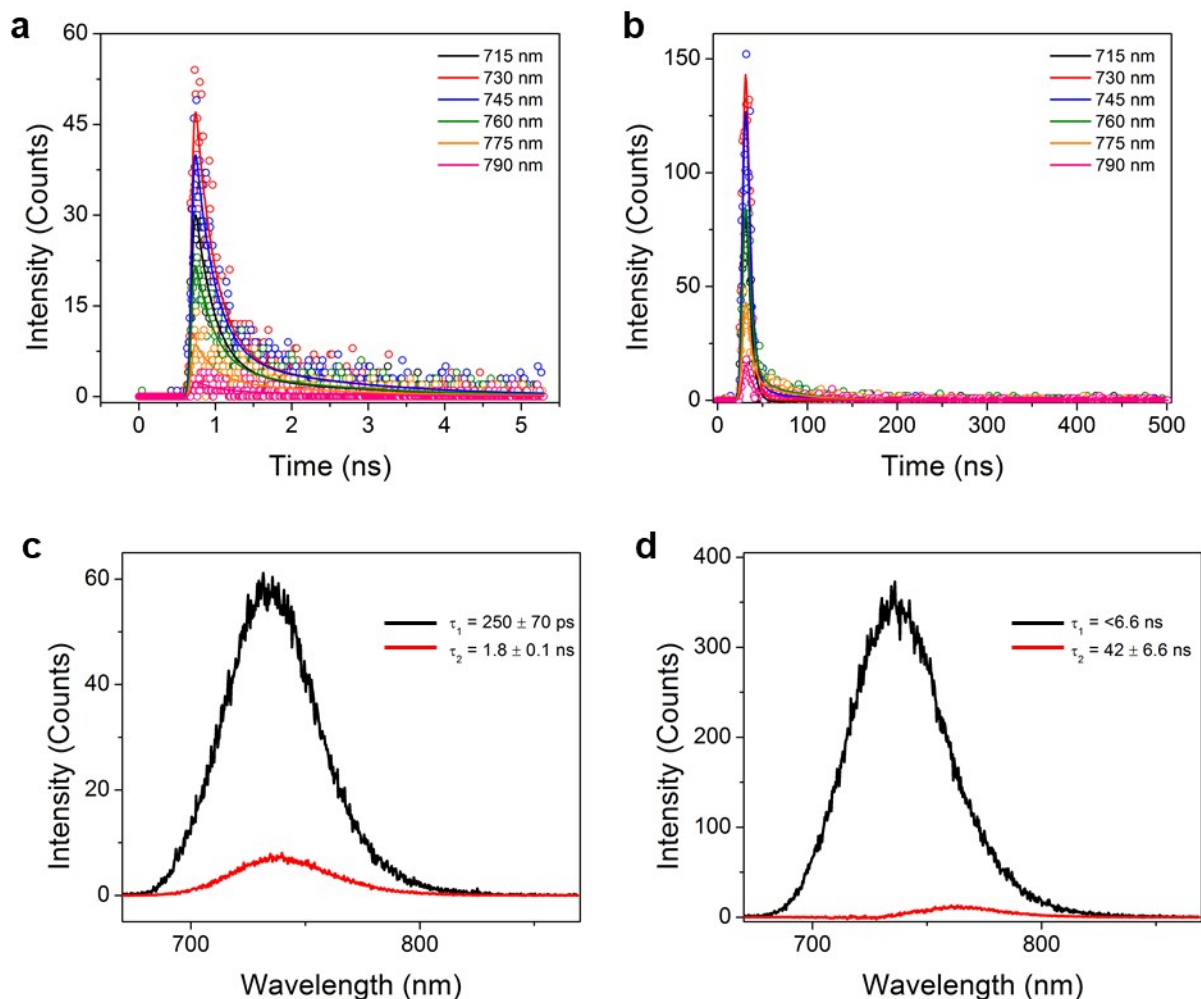
SI figure 13. XRD on 15:1 perovskite: PAA mass ratio thin films prepared a) with GBL/DMSO annealed 10 minutes at 120°C and 10 minutes at 100°C, b) with DMF/DMSO annealed 20 minutes at 100°C, and c) with DMF/DMSO annealed 10 minutes at 120°C and 10 minutes at 100°C.



SI figure 14. Steady-state-photoluminescence of the perovskite. The films were excited at 525nm. We observe that MAPbI₃ has a peak at 770nm, MAPbI₃-PAA and MAPbI₃-PEG have peaks at 760nm, while MAPbI₃-PVP has a peak at 730 nm.



SI figure 15. Time-resolved photoluminescence (TR-PL) of (a) MAPbI₃, (b) MAPbI₃-PAA, and (c) MAPbI₃-PEG. Single-wavelength kinetics at the steady-state PL peak for each sample were fit to a bi-exponential decay in all cases. We observe that PEG and PAA tend to increase the PL lifetime of the perovskite film.



SI figure 16. TR-PL data of MAPbI₃-PVP plotted as kinetic fits in (a) 5 ns and (b) 500 ns windows. These data sets were modeled with an A → B → ground model and the associated species-associated spectra are plotted in (c) and (d). The shorter time window (c) shows decay lifetimes (<2 ns) and emission spectra (peak at ~730 nm) comparable to the other samples. The longer time window (d) shows the fast decay process from (c) at ~730 nm which red-shifts (~765 nm) at later time points with a much longer decay lifetime (42 ns).